TouchpadAnyWear: Textile-Integrated Tactile Sensors for Multimodal High Spatial-Resolution Touch Inputs with Motion Artifacts Tolerance

Junyi Zhao
Meta Reality Labs Research &
Washington University in St. Louis
St. Louis, Missouri, USA
junyi.zhao@wustl.edu

Pornthep Preechayasomboon
Meta Reality Labs Research
Redmond, USA
prnthp@meta.com

Tyler Christensen
Meta Reality Labs Research
Redmond, USA
ctyler@meta.com

Amirhossein H. Memar
Meta Reality Labs Research
Redmond, USA
amirmemar@meta.com

Zhenzhen Shen
Meta Reality Labs Research
Redmond, USA
zzshen@meta.com

Nicholas Colonnese
Meta Reality Labs Research
Redmond, USA
ncolonnese@meta.com

Michael Khbeis
Meta Reality Labs Research
Redmond, USA
khbeis@meta.com

Mengjia Zhu
Meta Reality Labs Research
Redmond, USA
mengjiazhu@meta.com

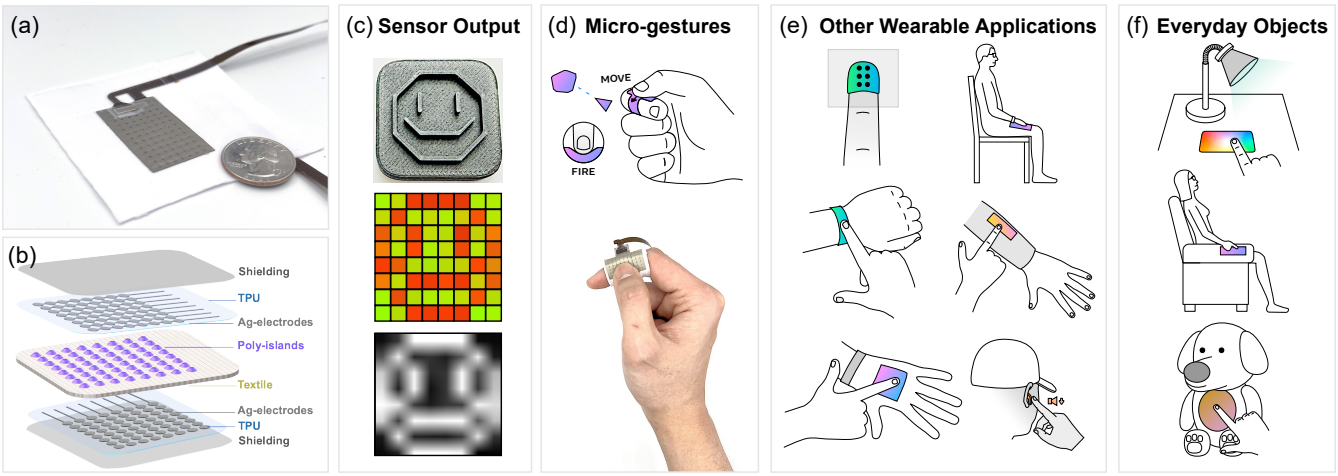

Figure 1: a) TouchpadAnyWear prototype featuring an 8×8 sensing pixel array. b) Schematic representation of the textile-integrated capacitive sensor array. c) Heat map illustrating analog values resulting from the application of a patterned stamp atop the sensor. d) Prototype showcasing a wearable finger sleeve designed for primitive thumb-to-finger gesture inputs. e) Examples of wearable embodiments include skin-interfaced tactile sensors on the fingertip, hand, and wrist, as well as laminated tactile sensors on soft and curved substrates such as garments and consumer electronics. f) Non-wearable embodiments encompass human-machine interactive interfaces integrated with everyday objects such as household appliances, furniture, and toys.

ABSTRACT

This paper presents TouchpadAnyWear, a novel family of textile-integrated force sensors capable of multi-modal touch input, encompassing micro-gesture detection, two-dimensional (2D) continuous input, and force-sensitive strokes. This thin (<1.5 mm) and conformal device features high spatial resolution sensing and motion artifact tolerance through its unique capacitive sensor architecture. The sensor consists of a knitted textile compressive core, sandwiched by stretchable silver electrodes, and conductive textile

UIST '24, October 13–16, 2024, Pittsburgh, PA, USA

ACM ISBN 979-8-4007-0628-8/24/10
https://doi.org/10.1145/3654777.3676344

shielding layers on both sides. With a high-density sensor pixel array (25/cm^2), TouchpadAnyWear can detect touch input locations and sizes with millimeter-scale spatial resolution and a wide range of force inputs (0.05 N to 20 N). The incorporation of miniature polymer domes, referred to as "poly-islands", onto the knitted textile locally stiffens the sensing areas, thereby reducing motion artifacts during deformation. These poly-islands also provide passive tactile feedback to users, allowing for eyes-free localization of the active sensing pixels. Design choices and sensor performance are evaluated using in-depth mechanical characterization. Demonstrations include an 8-by-8 grid sensor as a miniature high-resolution touchpad and a T-shaped sensor for thumb-to-finger micro-gesture input. User evaluations validate the effectiveness and usability of TouchpadAnyWear in daily interaction contexts, such as tapping, forceful pressing, swiping, 2D cursor control, and 2D stroke-based gestures. This paper further discusses potential applications and explorations for TouchpadAnyWear in wearable smart devices, gaming, and augmented reality devices.

CCS CONCEPTS

• **Hardware → Tactile and hand-based interfaces**; **Sensor devices and platforms**; • **Human-centered computing → Interaction devices**.

KEYWORDS

Touch Sensor, Tactile Display, Capacitive, Textile, Gesture Recognition, High Resolution, Soft Wearable, Fabrication, Printing, Motion Artifacts, Multimodal

ACM Reference Format:

Junyi Zhao, Pornthep Preechayasomboon, Tyler Christensen, Amirhossein H. Memar, Zhenzhen Shen, Nicholas Colonnese, Michael Khbeis, and Mengjia Zhu. 2024. TouchpadAnyWear: Textile-Integrated Tactile Sensors for Multimodal High Spatial-Resolution Touch Inputs with Motion Artifacts Tolerance. In *The 37th Annual ACM Symposium on User Interface Software and Technology (UIST '24), October 13–16, 2024, Pittsburgh, PA, USA.* ACM, New York, NY, USA, 14 pages. https://doi.org/10.1145/3654777.3676344

1 INTRODUCTION

Touch input technology is transitioning from traditional rigid hardware-integrated devices like keyboards, touchscreens, mice, and handheld controllers to more personal and mobile formats such as wearable electronics. The rapid growth in consumer adoption of intelligent mobile devices, exemplified by head-mounted displays (HMDs) and smart glasses, has driven the necessity of developing easy-to-carry wearable input devices for dynamic and on-the-go interactions, which is promising to enhance user experiences in Augmented and Virtual Reality (AR/VR) applications. Recent advancements have enabled the body itself to become a sensing platform through skin-interfaced soft electronics or integrations with wearable accessories such as smartwatches, wristbands, and rings. [6, 35, 36, 46]

Finger-based input is particularly promising for mobile touch interactions due to the fingers' intuitive and dexterous nature. Compared to mid-air gesture input methods [14], finger-based gestures, such as thumb-to-index finger pinching and thumb-on-index finger swiping, provide real-time haptic feedback and are less affected by environmental factors such as lighting conditions and visual obstructions. Various sensing mechanisms have been explored for finger-involved interactions. IMUs offer real-time motion tracking and compactness but may suffer from accuracy degradation over time and require periodic calibration [32]. Magnetic sensors provide robustness indoors but are vulnerable to external interference [27]. Optical sensors provide high-resolution tracking and robustness in diverse lighting conditions but require line-of-sight and complex algorithms for gesture interpretation [15]. Camera-based systems offer versatile gesture capture but consume more power and raise privacy concerns [30]. Amidst these technologies, mechanical force sensors, such as resistive or capacitive types, exhibit advantageous features for their reduced bulk, low power consumption, resilience against environmental interferences, and potential for integration with various substrates, which is promising in advancing the reliability and adaptability of interactive systems [7, 37, 41].

In this paper, we introduce TouchpadAnyWear (Figure 1), a series of wearable textile-integrated touch input interfaces featuring high-density capacitive sensor arrays for multimodal tactile sensing and gesture recognition. Compared to conventional wearable form factors in tactile sensing, such as ultra-thin epidermal electronics and bulk skin-interfaced electronics [13, 20, 21, 47], electronic textiles (E-Textiles) offer distinct advantages for developing mobile sensing and interactive interfaces [22, 23]. E-Textiles are characterized by their cost-effective fabrication, rendering them economically feasible for widespread adoption. Their soft and lightweight nature ensures comfort and minimal encumbrance during prolonged use, while their ubiquitous integration into everyday clothing maintains an unobtrusive appearance and seamless user experience [48]. E-Textiles also provide extensive customization capabilities, facilitating tailored sensor configurations to meet specific application needs.

The integration of tactile sensors into textiles introduces significant challenges that must be overcome to enhance their effectiveness and suitability for everyday applications. Seamless integration of tactile sensors with textile substrates is imperative to preserve comfort, durability, and aesthetic integrity. Additionally, the complexity of manufacturing processes and the compatibility of fabrication tools with textiles, as well as the potential for customizable, personalized, and scalable manufacturing solutions, must be addressed. Since high spatial resolution plays a pivotal role in precisely detecting and recognizing gesture inputs, thus ensuring resilience against motion artifacts induced by body movements or fabric deformations is important for maintaining consistent and accurate tactile sensing during dynamic activities.

The primary contributions of this paper are listed as follows:

- Design and construction of TouchpadAnyWear, a novel high-density capacitive sensor array (25/cm^2) integrated with textiles for high spatial resolution tactile sensing.
- Introduction and characterizations of the Poly-island methodology, a local stiffness programming approach designed to mitigate motion artifacts resulting from body movements and textile deformation.
- Development of a programmable and scalable direct-on-textile fabrication pipeline, allowing for customizable sensor configurations.

- Sensor data processing pipeline that captures 2D touch size, location, and pressure, for supporting micro-gestures, continuous 2D input, multi-touch, stroke-based gesture recognition, and text input.
- Design, user evaluation, and interaction explorations of two TouchpadAnyWear prototypes: a body-worn touchpad with a 8×8 pixel grid and a T-shaped finger sleeve for thumb-to-index finger interactions.

2 RELATED WORK

TouchpadAnyWear builds upon and intersects with several research areas in wearable input sensors. This section provides a concise overview of the existing literature on textile-based sensors and interaction designs. Table 1 presents an abbreviated list of prior work in wearable sensors for multi-modal touch input.

2.1 Textile-based Sensors

Textiles have emerged as a promising platform for constructing wearable electronics, seamlessly integrating functional electronic components like sensors, actuators, and circuits into fabrics to craft smart garments or accessories. This fusion of textiles and electronics offers numerous advantages, including enhanced flexibility, comfort, and breathability, making wearable electronics increasingly practical and convenient for everyday use. As a result, textile-based sensors have been developed in various form factors, such as patches [31, 51], finger sleeves [44, 45], and gloves [23, 37].

Several manufacturing techniques have been employed to add functional elements to textiles for sensing capabilities. For example, zPath [31] uses a piezoresistive material sandwiched between silver-plated ripstop fabrics to create hybrid resistive/capacitive sensors. TiMMi [44] consists of textiles coated with conductive silicone rubber for sensing finger pressure and bending. Sewing [12], embroidery [1, 39], and knitting [22, 23] are also commonly used in the manufacturing of textile-based sensors. In addition to the aforementioned techniques, various alternative approaches have been investigated to develop textile sensors. Scalable printing methods, such as screen printing [34, 48] and inkjet printing [4] have been explored to deposit conductive inks onto textiles. Additionally, laser cutting [2] could be employed to engineer fabrics with complex geometries, thus facilitating the creation of kirigami textile-based sensors.

Within the TouchpadAnyWear framework, textiles serve as the integral dielectric core of the capacitive sensing array rather than merely acting as supportive substrates, facilitating seamless integration across various wearable applications. By leveraging direct-ink-writing and layer lamination techniques, we have achieved precise direct-on-textile fabrication and expedited prototyping of high-density capacitive sensor arrays with efficiency. The entire fabrication process is compatible with existing tools, obviating the need for bespoke equipment and enabling broad adoption of this technique.

2.2 Interaction Designs

Textile-based wearable sensors have demonstrated their utility in a variety of touch interactions, notably including micro-gesture recognition and intuitive drawing for text input applications. Compared with conventional text input methods enabled by mocking sensors as keyboards [37, 41] for indirect text input, 2D handwriting for direct text input facilitates natural and intuitive interactions with augmented versatility on various objects, including the skin[40, 46]. Moreover, the use of 2D handwriting extends beyond text input, offering the potential for direct drawing and sketching capabilities, thereby expanding the possibilities within the realm of interaction design.

Multi-level force inputs with pressure sensitivity have emerged as an advanced feature in expanding the application capabilities of touch sensors [9]. For instance, PressTact incorporates three distinct levels of force input (light, medium, and strong presses) to facilitate bi-directional navigation tasks such as zooming, scrolling, and rotation [8]. Additionally, pressures leverage multi-level force input to enable implicit mode switching, thereby enhancing the functionality of multi-touch gestures on touchpads with rich capabilities [29].

With the capability to provide touch location, size, and force sensing through a high-density array format, TouchpadAnyWear enables all the interaction scenarios mentioned above with high spatial resolution and accuracy, including recognition of micro-gestures, 2D continuous input, multi-touch, as well as force-sensitive strokes, as illustrated in Figure 2. Additionally, the sensors have been textured to provide tactile feedback, enabling users to discern the precise locations of pixels without requiring visual focus, thus facilitating eye-free interaction.

3 SYSTEM OVERVIEW

TouchpadAnyWear is a new family of seamlessly integrated wearable touch-input sensors, featuring customizable high-density force sensor arrays, miniaturized plug-and-play sensing electronics, and a flexible input processing pipeline that can resolve 1D & 2D input with force sensitivity, and gesture recognition from sensing data for controlling user interfaces.

3.1 High-Density Sensor Array on Textile

The spatial resolution of a touch sensor array is an important parameter that determines the capability of micro-gesture recognition induced by subtle finger movements and the dynamic tracking of finger location in a 2D plane. Previous studies have reported resolutions of 1×3/finger [44], 2×2/patch [31], 7/finger [15] 2×4/finger [38], 3×3/nail [11]. In this paper, we demonstrated a sensor array with a higher density of 25 pixels/cm^2, totaling 8×8 pixels per device, thereby enabling the sensor to function in a versatile manner, akin to a laptop trackpad, for various gesture inputs.

3.2 Motion Artifact Tolerance

Motion artifacts pose a significant challenge for wearable touch sensors, potentially compromising sensor accuracy and reliability, and interfering with device functionality and user experience. In hand- or finger-interfaced wearables, such as gloves or finger sleeves, natural hand and finger movements, as well as skin deformations, introduce unwanted signals and noise [18]. As illustrated by the parallel plate capacitor equation $C = \frac{\varepsilon \cdot A}{d}$, changes in gestures lead to fabric deformation, which in turn alter the distance (d) and

Table 1: Prior work in wearable sensors for multi-modal touch input

	Form Factor	Sensing Mechanism	Density	Touch Input				Examples
				B.C.	A.F.	1D	2D	
This work	various (e.g. finger sleeve, textile patch)	capacitive	25/cm^2 (up to 64/phalange)	✓	✓	✓	✓	micro-gestures, stroke-based gestures, multi-touch, joystick, text entry (handwriting)
TouchLog [15], 2023	fingernail-type	photo-reflective	7/fingertip	✓	×	✓	✓	micro-gestures
TipText [41], 2019	fingertip	capacitive	5/cm^2	✓	×	×	×	text entry (keyboard)
ThumbRing [32], 2016	ring	IMU	1/finger	✓	×	✓	×	slider, touch
Fingerpad [6], 2013	nail-mounted	magnetic	9/nail	✓	×	✓	✓	cursor control
HandSense [26], 2019	glove	capacitive	1/finger	✓	×	✓	×	micro-gestures
DigiTouch [37], 2017	glove	resistance	1/finger	✓	✓	✓	×	text entry (keyboard)
TIMMi [44], 2015	finger sleeve	piezoresistive	3/finger	✓	✓	✓	×	micro-gestures
iSkin [36], 2015	skin-worn	capacitive	5/finger	✓	✓	✓	×	sliders or click wheels
FingerInput [30], 2018	shoulder mount	depth sensing	1/shoulder	✓	×	✓	✓	micro-gestures
zPatch [31], 2018	eTextile patch	R/C hybrid	4/patch	✓	✓	✓	×	sliders
NailO [11], 2015	nail-mounted	capacitive	9/nail	✓	×	✓	✓	remote controller
SkinTrack [46], 2016	wristband & ring	wave propagation	1/hand	✓	×	✓	✓	sliders, drawing
Iontronic Panel [40], 2023	sleeve	capacitive	1/arm	✓	×	✓	✓	drawing, handwriting

Touch Input: B.C.= binary contact, A.F. = analog force, 1D = one-dimensional slider, 2D = two-dimensional input.

alignment area (A) between the electrodes. Two strategies—poly-islands and kirigami design—have been employed in this work to mitigate motion artifacts in textile-integrated capacitive touch sensors, thereby enhancing their usability and robustness in real-life applications.

3.2.1 Isolated "Poly-islands" for strain-locking purposes. Encapsulating textiles with silicone has been reported as an effective method to mitigate motion artifacts [25, 42, 43]. However, employing a full-area composite significantly alters textile's physical properties, compromising its inherent characteristics such as softness, breathability, and conformability. Here, we introduce a strategy that employs isolated silicone "islands" patterned onto textiles to achieve strain-locking through local structural confinement. Under universal deformations (e.g. bending, stretching), the structural elongation predominantly occurs in the non-coated pristine regions, while the poly-islands substantially constrain the distortion of active sensing pixels. This technique effectively enhances motion-artifact tolerance by redefining the strain distribution within the textile. Furthermore, the poly-islands can serve as markers, enabling eye-free mobile inputs by guiding users' fingers to discern the precise locations of pixels and the distance of finger movements for micro-gesture inputs.

3.2.2 Kirigami design by laser-engraved openings. The incorporation of multiple functional layers, such as electrodes, shielding, bonding, and encapsulation, in skin-interfaced sensors often restricts natural hand and finger flexibility and compromises wearing comfort [10, 31, 37]. To mitigate this issue, we employ a laser cutter (LPKF ProtoLaser R4) to engrave structural openings on electrode and shielding layers. By strategically designing the pattern and layout of these openings, deformation can be precisely oriented and redistributed to prevent distortion of the active sensing regions (refer to the following "Motion Artifacts Tolerance" discussion in Section 6.2). This approach offers a secondary resilience against motion artifacts while preserving maximum mechanical flexibility and minimizing encumbrance.

3.3 Wearable Form Factors

Various form factors have been explored to evaluate the universal effectiveness of devices in everyday applications. By employing modular design concepts and scalable fabrication pipelines, device shape, size, layout, and spatial resolution can be readily adjusted and customized according to specific needs.

3.3.1 Miniaturized textile trackpad for touch input. A 1×1 $inch^2$ textile patch can accommodate a total of 64 (8×8) active sensing pixels, functioning akin to a laptop trackpad for diverse interactions.

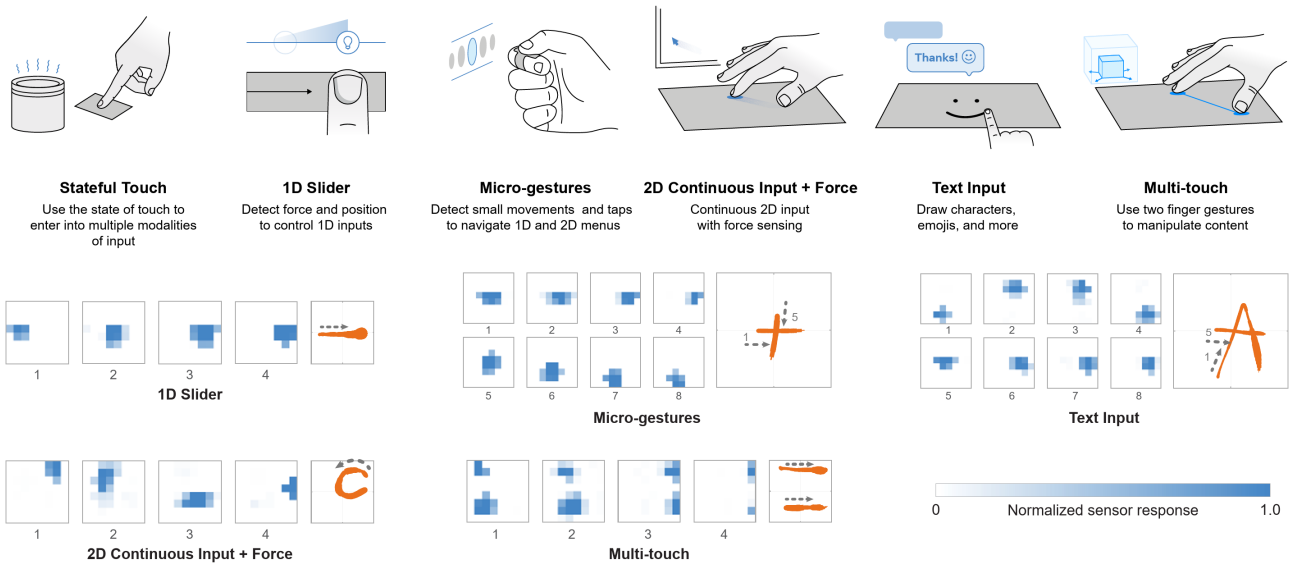

Figure 2: Example interactions possible with TouchpadAnyWear and their corresponding sensor data and processed strokes. Sensor data is presented as normalized values on an 8 by 8 pixel grid in snapshots over time. The rightmost plot of each interaction is the processed stroke with the arrow indicating the start and number corresponding to the starting snapshot. The stroke's width indicates the force sensed.

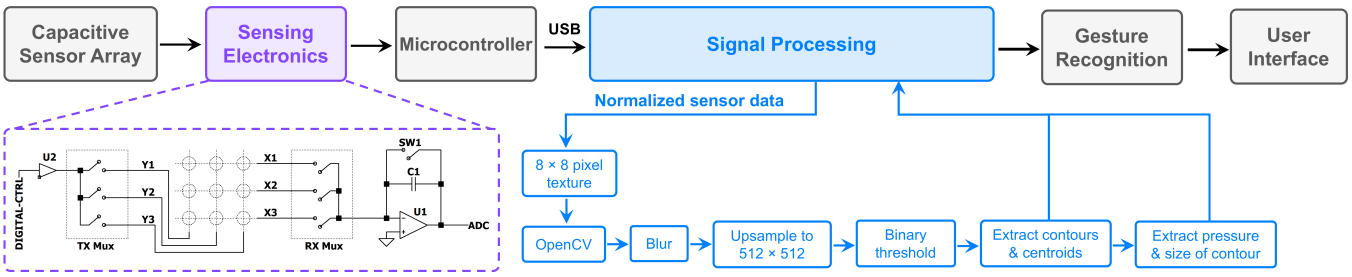

Figure 3: Block diagram of TouchpadAnyWear system with the detailed electronic circuit design and software data processing pipeline

These interactions include tap (light, hard), swipe (left, right, up, down), continuous 2D cursor movement, and text input. Such a miniaturized textile touchpad holds the potential to function as a standalone gesture input device or seamlessly integrate with garments for everyday wearables. For instance, it can be sewn as into gloves or wristbands to facilitate immersive interactions, or stitched inside pockets of clothing for discreet interactions.

3.3.2 Finger sleeve for thumb-to-finger gesture recognition. Finger-worn sensors offer a promising form factor for mobile interactions, aligning well with the dynamic movements of fingers [44, 45]. The interaction between a bare thumb and a ring-like sleeve worn on the index finger allows natural, unencumbered gestures without compromising fingertip dexterity during daily activities. In addition to typical gesture inputs such as tap (light/hard) and swipe (left/right/up/down), the sensor's high spatial resolution enables the detection of subtle motion trends, facilitating recognition of rich micro-gestures triggered by subtle local movements of the thumb.

3.4 Hardware

The sensing electronics (Figure 3) consists of two banks of analog multiplexers, one for each sensor axis, allowing for any sensor pixel to be attached to the acquisition system at any time. To sample a region, SW1 briefly closes to discharge the integrating capacitor C1. A rising or falling edge is driven out of the TX Mux by U2, and the amplifier U1 integrates the charge accumulated through the sensor capacitor which is proportional to capacitance. After the amplifier has converted this integrated charge into an output voltage, an analog-to-digital converter (ADC) samples the output of U1 after the settling time elapses. This cycle repeats selecting each pixel one-by-one and sampling the capacitance to scan the entire grid.

The sampling rate is limited by the performance of the analog processor used for sampling. In the data acquisition implementation in this paper, the system is capable of sampling approximately

1,200 pixels per second. This electrical sensing architecture is immune to parasitic capacitance to ground on both the transmitter and receiver sides, allowing for shielding interconnections and the sensors themselves with a simple connection to the ground rather than requiring a driven shield.

3.5 Software

The sensing hardware in the previous section transmits the sensor readings to be processed on a PC in real-time using serial communication via USB. In this paper, the Unity game engine, along with OpenCV [3] is used to process the incoming readings for driving user interface mock-ups and performing user studies as described in the following sections (Figure 3).

With the approximate location, size, and amount of force being pressed on the sensor area as the desired output, the processing pipeline first takes the raw samples and normalizes the signals using a predetermined baseline and maximum reading. The normalized value is then converted into an 8×8 pixel grayscale image.

The OpenCV library is used to first perform a Gaussian blur with a 3×3 kernel on the raw image, followed by upsampling to 512×512 pixels using bicubic interpolation. Then binary thresholding segments portions of the image with higher values, which signify pixels that are being actively pressed. This threshold is configurable, but is constant at 0.2 throughout the studies and demonstrations explained in this paper. Then, all contours on the thresholded image are used to calculate the size and centroid of each contiguous region of pixels, with the largest region considered the actively pressed region. The grayscale values under the region of interest are sampled and used to calculate the overall pressure by taking the sum of pixel values divided by the total pixel area. This provides 1) the centroid of the pressed location, 2) the size of the area being pressed, and 3) the amount of pressure under that area. Pressure and size can be used to estimate overall force, or pressure can be used directly depending on the interaction. All steps are performed within one frame of the Unity application, which runs at approximately 90 frames per second. From the aforementioned data, meaningful inputs can be derived as follows:

3.5.1 Stateful Touch. Stateful touch is defined when the user is actively interacting with the sensor. Using the size of the area being pressed, this state is defined by using a predetermined threshold to enter the state and a lower threshold to exit the state. This is the basis for all subsequent interaction modalities, meaning that stateful touch is used to signify the beginning and end of each interaction.

3.5.2 Micro-gestures. Micro-gestures in this paper are defined users drawing a short stroke in cardinal directions on the sensor to navigate a user interface. First, a 1-Euro filter [5] is applied to the location with the parameters fcmin = 5, derivative cutoff = 1, and beta = 0.07. Then, using the pressed location over time and stateful touch, the system can determine whether the user is swiping towards the Left, Right, Up or Down from their starting point. If the user does not move their finger from the initial location, under a certain threshold, and within 350 milliseconds, then the gesture is a Tap. Using this protocol, five distinct gestures (Left, Right, Up, Down and Tap) can be derived from the sensor. If certain form-factors of the sensor are not suitable for some gestures, such as Up and Down when swiping perpendicular to a narrow strip, then those gestures can be disabled (as in the case of the finger-worn prototypes shown in subsequent sections).

3.5.3 Stroke-based Gestures. Stroke-based gestures are defined as a series of strokes that the user can draw on the sensor area to be used as shortcuts, such as drawing a checkmark for completing a to-do list item, or as text input by directly drawing the letter. Strokes that the user performed can be continuously collected by recording the tracked locations of the pressed area over time. Once the user has stopped applying force to the sensor for a certain amount of time (1 second is used in the user studies and demonstrations), the strokes are processed using the $Q Recognizer [33] and recognized against a set of pre-trained gestures (templates).

3.5.4 2D Continuous Input. The location of the finger can be continuously tracked to drive a cursor, while using stateful touch to signify active interaction. The tracked location is first filtered using a 1-Euro filter with the parameters fcmin = 2, derivative cutoff = 0.5, and beta = 0.007, then the location of the 2D cursor can then be calculated on a per-frame basis by multiplying the change of location with an acceleration gain from a curve mapped to the distance from the previous frame to the current frame and then adding the resulting vector to the current cursor position. A Tap gesture is used as a confirmation or click. Aside from the virtual cursor drawn on the application's screen, the cursor of a Windows PC can be driven from Unity to utilize external software for user studies and for demonstration purposes. Furthermore, for continuous 1D input, one of the dimensions can be isolated from the 2D input or disabled altogether.

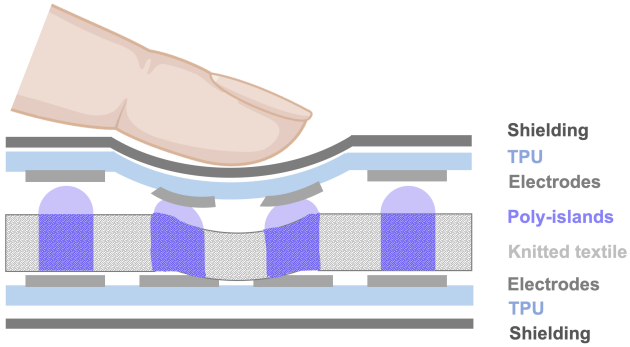

Figure 4: a) Schematic of textile-integrated capacitive sensor architecture.

4 DESIGN CHOICES

The capacitive sensor is composed of an elastic knitted fabric with patterned poly-islands serving as the core, which is sandwiched between stretchable electrodes (Figure 4). The device is shielded by the outermost conductive fabric tapes, which are in direct contact with human skin. The sensor is connected to circuitry hardware for data acquisition, and a user-friendly software interface was developed for multi-channel data readout and real-time display.

4.1 Poly-islands

Bluesil RTV 3040 silicone rubber was chosen to fabricate poly-islands due to its advantageous properties. The extended pot life of 2 hours provides ample time for material processing and enables the production of intricate and large-scale patterns in a single session. The high viscosity of 50,000 cP aids in the creation of fine features by minimizing bleeding among the fibers before complete curing. With a Shore A hardness of 38, the silicone offers a stiffness that is an order of magnitude higher than the pristine textile. The high modulus enhances strain-locking effectiveness, thereby improving tolerance to motion artifacts.

4.2 Knitted Textiles

To optimize sensitivity and broaden the response range of the tactile sensor, three types of textiles with varying compositions, knitting structures, and thicknesses were evaluated. Among them, *Fabric-3*, a blend of 86% polyester and 14% spandex with a thickness of approximately ~900 μm, was selected due to its superior elasticity and inherently largest compression displacement. *Fabric-3* demonstrated a compression displacement of nearly 70% under a 10 N force, offering substantial compressible space along the Z-axis, which is important for altering capacitance in response to touch input (Figure 5). Furthermore, the integration of poly-islands was validated to enhance sensor performance by increasing the compression capability of the composite dielectric core while reducing hysteresis during reversible response. This improvement enabled an approximate displacement of 80% under the same 10 N force, further augmenting the sensor's responsiveness and reliability.

4.3 Stretchable Electrodes

Stretchable silver ink (SS1109, ACI Materials) was chosen for fabricating intrinsically stretchable electrodes and interconnects. Compared to other reported elastic conductors, such as conductive polymer PEDOT:PSS [19–21], metal nanowires [49, 50], carbon-filled silicone [36], and liquid metal [24], the selected silver ink offers superior adhesion to thermoplastic urethanes (TPU) films, excellent conductivity, and compatibility with various patterning methods, such as screen printing and syringe dispensing.

4.4 Shielding Material

The selection of conductive fabric tape (5113FT, 3M) as the outermost encapsulation layer fulfills the dual purposes of grounding and electromagnetic interference (EMI) shielding. With a thickness of 50 μm, this material is optimal for the tactile sensor, allowing for safe direct skin contact while also providing a desirable fabric texture.

5 MANUFACTURING PROCESS

The step-by-step fabrication process of the TouchpadAnyWear is illustrated in Figure 6.

5.1 Textile Core with Poly-islands

Silicone rubber was prepared using a vacuum mixer at a mix ratio of A:B=10:1. A 3-axis automated fluid dispensing robot (Nordson EFD) was utilized to deposit the silicone onto the textile surface.

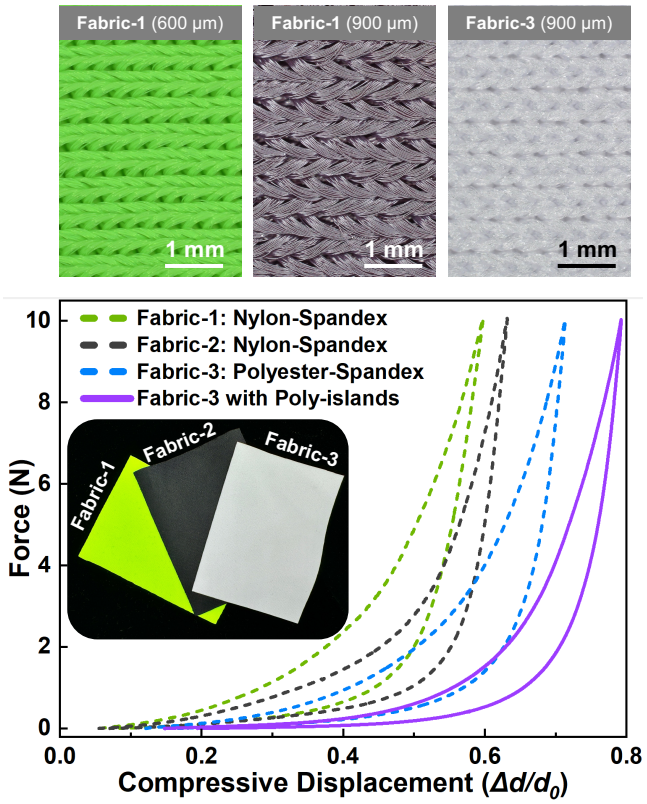

Figure 5: Characterization of various dielectric core materials

A 25-gauge dispensing tip was chosen to ensure precise control over the deposition of silicone droplets, achieving the feature size of poly-islands at sub-millimeter dimensions. The robot executed the programmed layout automatically, and the samples were subsequently cured at 120 °C for 10 minutes. The device's size and layout are highly scalable through programming the pixel dimensions, pitch size, and individual pixel locations using the dispensing robot, which has a maximum working area of 350 by 350 mm.

5.2 Stretchable Silver Electrodes

The same dispensing robot was utilized to pattern stretchable silver ink onto a TPU film, employing a 27-gauge dispensing tip. Optimization of the moving speed and the spacing between the tip and the TPU film was critical to achieve silver traces with the desired thickness, ensuring the fabrication of durable electrodes with high conductivity. Following the patterning process, the samples were air-dried for 20 minutes in ambient conditions before undergoing a 5-minute curing process in an oven at 120 °C. The widths of the silver traces were maintained within 300 μm. As depicted in Figure 6, the resistance of the printed electrodes exhibited robust mechanical stretchability, enduring up to 50% elongation with consistent performance and low hysteresis, ensuring reliable conductivity of the stretchable conductors. Finally, the TPU film with patterned silver electrodes underwent laser trimming and engraving to achieve designed kirigami patterns before bonding with a Flexible Printed

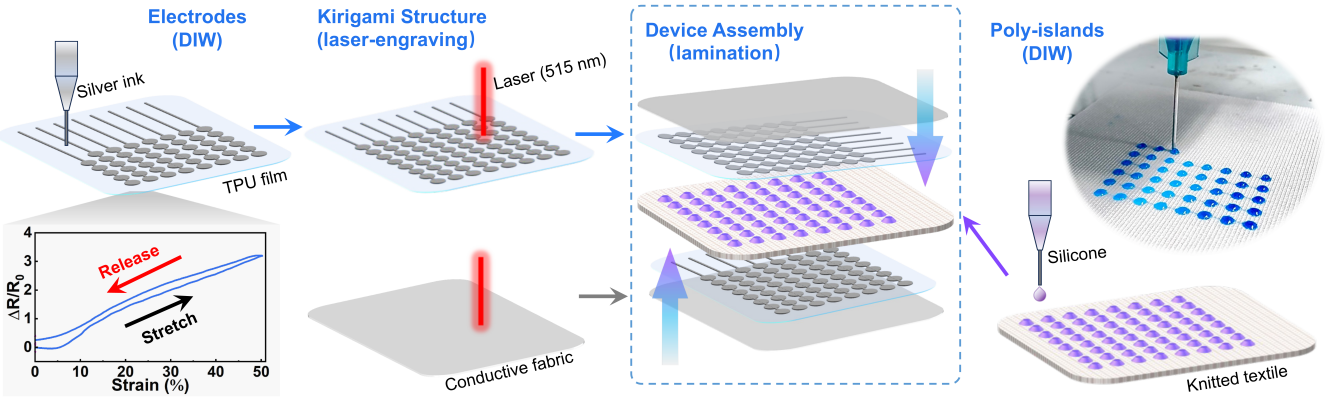

Figure 6: Fabrication process of the 8 by 8 pixel tactile display.

Circuit (FPC) using Anisotropic Conductive Film Adhesive (7303, 3M).

5.3 Sensor Assembly

The prepared components, including the textile dielectric core and stretchable electrode films, were assembled into a sandwich structure through lamination, aided by laser-engraved fiducials. Prior to lamination, the conductive fabric tape was laser-engraved with the desired kirigami design and trimmed to match the shape of the electrode film. Subsequently, shielding fabric films were affixed to the outermost sides, connecting with the grounding pad on the Flexible Printed Circuit (FPC). Encapsulated within TPU and shielding layers, the electrodes are protected from direct exposure, ensuring durability for spot cleaning of the devices. Once integrated, the device is ready for use upon connection to the circuit board described in Section 3.4.

6 DEVICE CHARACTERIZATIONS

6.1 High Sensitivity Sensor Pixel

The sensitivity of individual sensor pixels is critical for developing tactile displays that can render subtle and primitive touch interactions necessary for micro-gesture recognition and everyday applications. As shown in Figure 7, the sensor pixel demonstrates the ability to detect a broad range of force inputs, from 0.05 N to 5 N. During cyclic tests at each load, a residual force of approximately 10% was preset to prevent the testing instrument (Instron) from resetting to an absolute-zero input. Furthermore, the reliability of the device under dynamically varied inputs has been validated. As shown in the lower panel of Figure 7, the applied force was simultaneously monitored using a force gauge placed beneath the sensor. The tests began with typical interactions, such as tapping and swiping (~2.5 N), followed by the application of maximum normal force (~20 N) both steadily and dynamically. Throughout these tests, the sensor exhibited robust performance without any signs of degradation or damage. This extensive response range accommodates diverse interaction modalities with varied force inputs, thereby broadening the spectrum of tactile interactions.

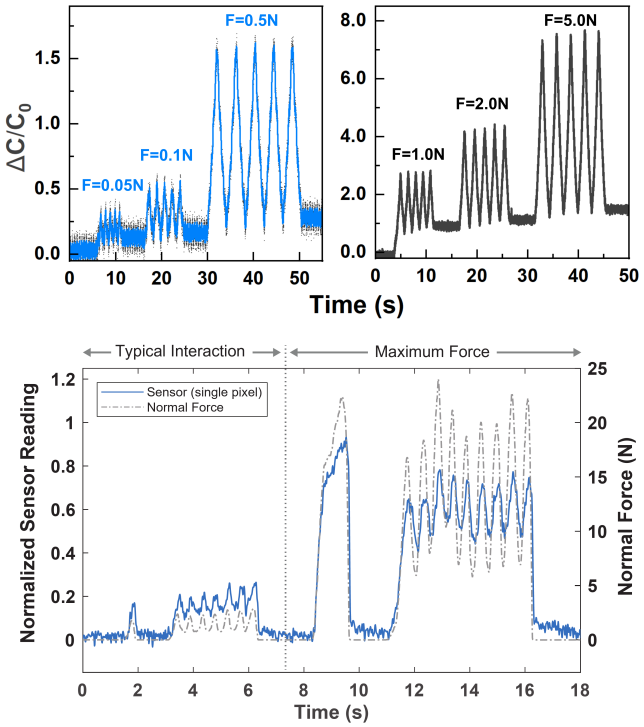

Figure 7: Top: Capacitive responses of a single pixel under a wide range of force inputs from 0.05 N to 5.0 N, with 5 cycles repeated at each load. Top-Left: fitting plots (blue curves) of raw data (back dots) under 0.05 N, 0.1 N, and 0.5 N force inputs; Top-Right: plots of raw data under 1.0 N, 2.0 N, and 5.0 N force inputs. Bottom: Simultaneous readings from a single sensor pixel and a force gauge during dynamically varied force inputs ranging from 0 to 20 N.

6.2 Motion Artifact Tolerance

Both the implementation of poly-islands and the laser-engraved openings contributed to mitigating motion artifacts in the device:

1) *Poly-islands.* To visually assess the strain-locking effectiveness facilitated by the poly-islands, the textile underwent stretching by 20% and 40%, during which the actual deformation in regions with and without poly-islands (dyed blue using pigment) was quantified. As depicted in Figure 8a, when stretched by 20%, the knitted structure covered with silicone exhibited a mere 2% elongation compared to a 22% deformation in the untreated surrounding area. Upon stretching by 40%, the poly-island region exhibited remarkable resilience, with only a 5% elongation observed, contrasting starkly with the 44% deformation in the surrounding region.

2) *Kirigami design by laser-engraving.* The openings were engraved into perpendicular narrow sleeves (100 μm) to ensure biaxial deformation flexibility in wearable contexts while preserving the shielding effectiveness. The arrangement of these sleeve openings was strategically designed surrounding the active sensing pixels to guide the orientation of creases, thus preventing interference with the sensing pixels and facilitating the redistribution of strain throughout the device (Figure 8b).

The practical tolerance to motion artifact was assessed by evaluating the baseline drift of the sensor at zero input during vigorous bending deformations. Under a 30°bending, the experimental sample (sensor equipped with poly-islands and engraved openings) demonstrated a capacitance change of less than 1.5%, while the control sample (sensor without poly-islands or engraved openings) exhibited a significantly higher drift over 5%. Upon complete perpendicular folding to 90°, the experimental sample showed an approximate 2.5% change compared to nearly 10% in the control group. Furthermore, upon returning to its pristine state, the experimental sample exhibited immediate recovery without observable capacitance offset, unlike the control sample displaying an unrecoverable change.

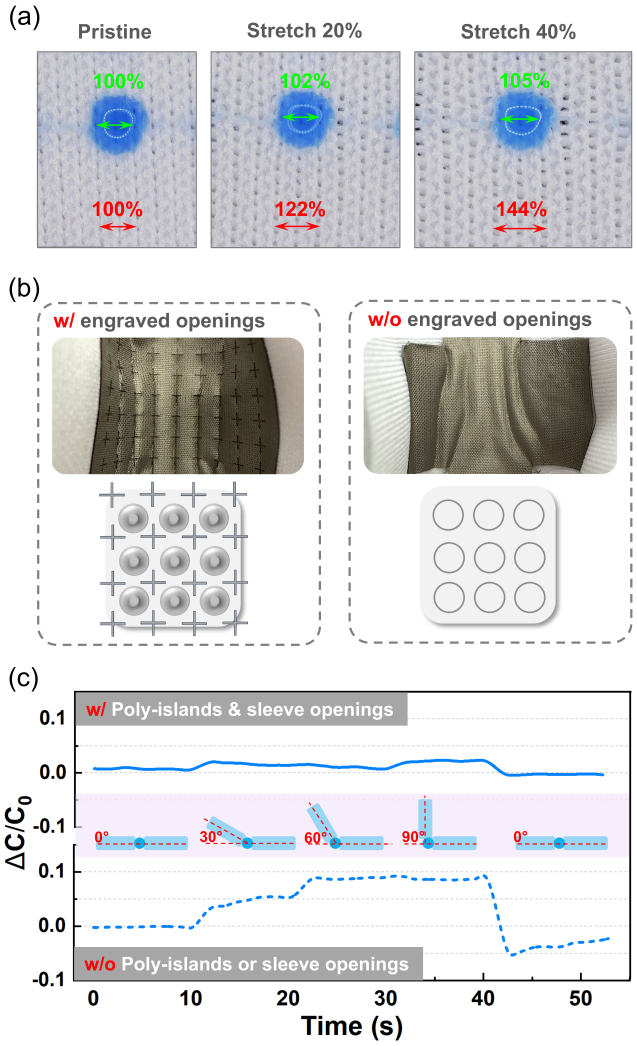

Figure 8: a) The strain-locking effect of poly-islands during device stretching. b) Laser-engraved sleeve openings on electrode and shielding layers for oriented deformation. c) Baseline drifting comparison of tactile sensor displays with and without poly-islands and sleeve openings under varied bending degrees.

7 EVALUATION

To determine the efficacy of gesture recognition and 2D continuous input, three user studies were conducted, each focusing on a specific input modality: 1) Simple gestures, 2) Stroke-based gestures, and 3) 2D continuous input. TouchpadAnyWear in an 8 by 8 pixel configuration was evaluated with the sensor adhered to the participants' pants on the lap area, where it was comfortable for interacting with their dominant hand. Participants were encouraged to behave naturally during the user studies, with no restrictions imposed on their movements. The sensor was securely taped to the participants' pants, ensuring that clothing deformation and body movements were synchronized with the device. This setup aimed to validate the sensor's robustness against various deformations in practical application scenarios. Each study was run using the Unity application on a laptop, with the laptop's screen displaying the studies' user interface. The user study flow was authored and controlled using the Bricklayer[28] package for Unity. Demonstrations of all user studies are shown in the accompanying video.

7.1 Micro-gestures

To evaluate the sensor's gesture recognition capabilities, we recruited 25 participants (12 male, 13 female) from our office. Participants were industry professionals of varying backgrounds such as research scientists, software engineers, electrical engineers, and research assistants. Each participant was asked to perform a total of 50 gestures, consisting of 10 repetitions of each of the following: Left, Right, Up, Down, and Tap. Each study starts with participants first wearing the sensor on their lap. Participants are prompted to do each gesture using icons shown in Figure 9. After practicing each gesture 3 times, participants are given a chance to try out any gestures missed during practice. Participants then perform the gestures in a randomized order as shown on the screen. The recognition system provided immediate feedback: a brief flash of green if the gesture was correctly detected, and a brief flash of red if it was not. The completion time for each gesture and the recognized

gesture were recorded. Each study session took approximately five minutes to complete.

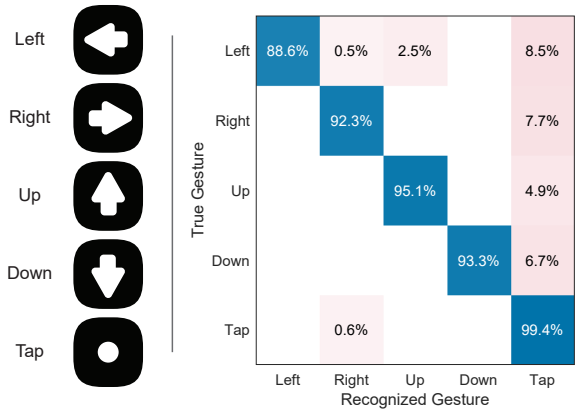

Figure 9: Left: Icons shown as prompts to users to perform gestures. Right: Confusion matrix showing the accuracy of each recognized gesture from the user study.

The results from the study shows that the system as a whole has a mean accuracy across all gestures of 93.7% with the Left gesture having the lowest accuracy of 88.6% and the Tap gesture having the highest accuracy of 99.4%, as shown in Figure 9. The median time to complete any gesture across all participants is 1.05 seconds from the time the gesture is shown up until the gesture is performed and recognized.

From observations during the user study, the higher error rate of all gestures aside from Tap can be attributed to strokes that are too short to be recognized as directional and are misclassified as Taps, which is also apparent in Figure 9. Subjective comments collected during the study revealed that some users were used to the capacitive touchpad of a laptop or touchscreen, where only minimal force is required, whereas TouchpadAnyWear requires a small amount of force to register (P21: "I feel like I have to swipe a little bit harder than I would like to"). Regardless, despite the simplicity of the gesture recognition algorithm, the sensor provided high accuracy for gesture recognition, and can be improved by either increasing the sensor's sensitivity (e.g. reducing force required to register stateful touch) or using more robust algorithms.

7.2 Stroke-based Gestures

The purpose of evaluating stroke-based gestures is twofold: 1) to evaluate the sensor's capability to resolve two-dimensional strokes on the active sensing area, and 2) to evaluate the efficacy of the sensor's use for personalized, repeatable stroke-based gestures. 10 participants (4 male, 6 female) of the 25 participants of the previous study were recruited to participate in a user study, where they were using their index finger on their dominant hand to draw on TouchpadAnyWear on their lap, of their own interpretation of drawings shown on the screen. Strokes are recognized using the $Q Recognizer as detailed in Section 3.5.3. The set of eight gestures are as follows: Check, Circle, Cross (X), Frown, Heart, Question, Smile, and Wipe, and are presented to the user as shown in Figure 10.

First, participants are asked to draw 4 sets of each gesture as templates for the recognizer followed by a chance to practice the drawings for a brief period with feedback given on what each drawing is recognized as. Then, participants were given a randomized order of all 8 gestures, each for 8 repetitions, totaling 64 trials, to perform. The strokes performed, including pressure and size used, and raw sensor data, were collected along with the recognized gesture. The participant receives feedback whether the gesture was recognized correctly similar to the previous user study.

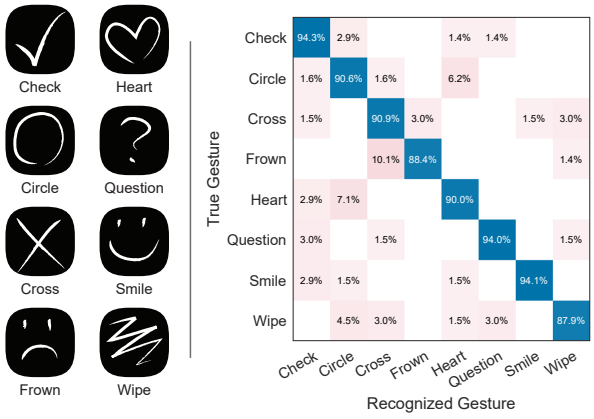

Figure 10: Left: Icons that were presented to the user to record their interpretation of the gesture as templates for the gesture recognizer. Right: Confusion matrix showing the accuracy of the recognized personalized gestures.

The results show that across all stroke-based gestures, the recognition achieved an accuracy of 91.3%, with the Wipe gesture having the lowest accuracy at 87.9%, as shown in Figure 10. Of note, the highest confusion was between Frown and Cross, and Circle and Heart.

Upon further analysis of the recorded strokes, some Frowns were recognized as Crosses due to participants not reducing enough force between strokes, while some participants drew incomplete Hearts which were misinterpreted as Circles. The error could also be possibly explained by the geometric similarities between a heart and a circle. The Wipe gesture's lower accuracy is believed to be due to the complexity of the gesture itself and some participants preferring to draw smaller and shorter Wipes which do not have enough spatial information to discern between other gestures, as shown in some of the examples in Figure 11.

7.3 2D Continuous Input

To evaluate the efficacy of the sensor as a 2D continuous input device (trackpad), the same 25 participants from the first study were also recruited to perform a Fitt's law study by interacting with TouchpadAnyWear on their lap. The laptop's cursor is controlled using synthesized mouse inputs via Win32 application programming interface (API) calls, where click events are driven using the Tap gesture. The FittsStudy [16] application was then used to run

the user study and collect data, which uses the emulated mouse as input. The study consists of two sections: 1D and 2D Fitt's law pointing tasks each with amplitudes 256, 384, and 512 pixels and widths 64, 96, and 128 pixels, totaling 9 repetitions across 9 configurations per section (81 trials per section). The laptop's screen is 15.6 inches measured diagonally and has a resolution of 1920 by 1080 pixels. Each section takes approximately 8 minutes to complete.

The results from the study show that the sensor in 2D continuous input mode can achieve a mean throughput of 0.96 bits/second for the 1D task and 0.87 bits/second for the 2D task. Upon closer analysis, trials with the widest amplitude (512 pixels), had a higher mean throughput of 1.02 bits/second and 0.97 bits/second for 1D and 2D respectively, compared to the lowest amplitude (256 pixels) at 0.83 bits/second and 0.73 bits/second for 1D and 2D respectively. This suggests that perhaps the control-to-display ratio was set too high (in this case, the cursor's acceleration) and improvements can be made by adjusting this on a per-user basis.

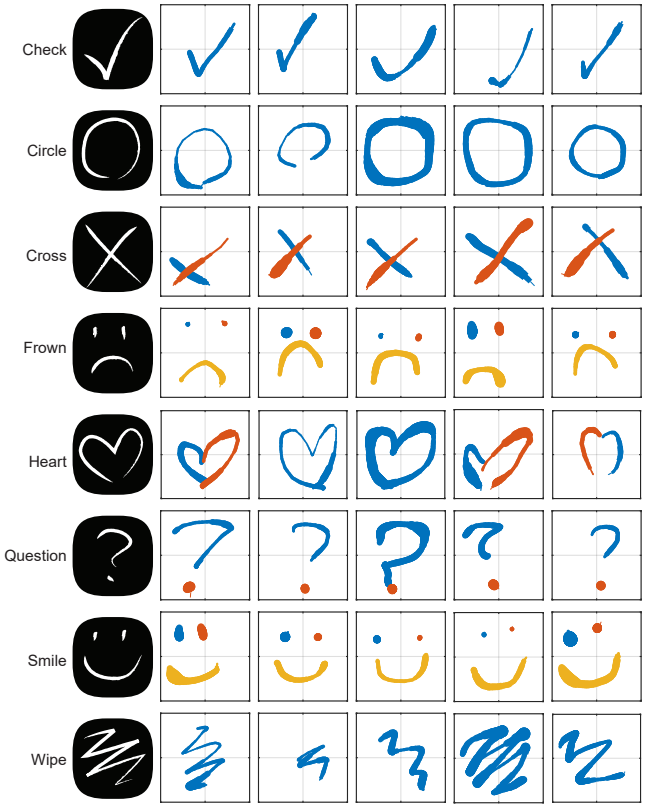

Figure 11: A collection of personalized gestures collected during the user study across various participants. Each color represents one continuous stroke and the amount of force is shown as each stroke's width.

7.4 Subjective Feedback

After each user study concluded, we asked for unstructured feedback from participants about their experience with the device. Some participants noted that the bumpy texture and tactile feedback were unobtrusive and gave generally positive feedback about the feel of the texture (P7, P11, P22, P24). Some participants noted the robustness and versatility of the sensor for various applications (P1, P13, P23). However, some participants were surprised by the amount of force required to register during the cursor task (P17, P20), when probed further, the cause was their familiarity with capacitive trackpads found in laptops that require miniscule amounts of force.

8 INTERACTION EXPLORATIONS

Using the rich information from the sensing area: touch location, size, and pressure, and the interactions outlined in the user studies as building blocks, this section extends the interactions into short demonstrations. A finger-worn prototype is also introduced which utilizes a subset of the interactions offered by the lap-worn prototype. Readers are highly encouraged to refer to the video accompanying this paper for full demonstrations of the following interactions.

8.1 Finger Sleeve Prototype

Due to the textile nature and integrability of the sensor, a finger sleeve prototype was fabricated by rolling the textile into a tubular shape able to fit on the middle phalanx of the index finger, as shown in Figure 1 and Figure 12. The intention is for the user to perform micro-gestures, continuous directional input and continuous force input on the sensor.

8.2 Text and Emoji Input

In this demonstration, the gesture recognition system introduced in Section 3.5.3 is extended to support text entry by adding templates for the entire alphabet. The Smile and Heart gestures are used for inputting a "Grinning Face" emoji and a "Smiling Face with Heart-Eyes" emoji (Figure 12a). A Wipe gesture is used to delete text. This interaction is demonstrated using the on-lap prototype.

8.3 Navigation Micro-gestures

Using the gestures introduced in Section 3.5.2, a grid of items is presented to the user that can be browsed using the Up, Down, Left, Right and Tap gestures. Each cardinal gesture moves the selector along its direction, while the Tap gesture is used for selection. All four cardinal directions are demonstrated on the on-lap prototype (Figure 12b), while the finger-sleeve prototype supports the Left, Right, and Tap gestures for a single-dimensional list of items.

8.4 Continuous Input

As introduced in Section 3.5.4, the touched location tracked over time can be used to emulate a cursor (two-dimensional) or modulate a single value (one-dimensional). In the demonstration for the on-lap prototype, a joystick is presented to the user (Figure 12c) where the continuous 2D input is used to pull the joystick in any direction, once the user lets go, the joystick knob springs back to its original position. In the demonstration for the finger-sleeve prototype, a bar that responds to the X-axis of the cursor is presented to the user (Figure 12d). Aside from sliding their thumb over the sensing area, users can also press down slightly and roll their thumb to perform small adjustments instead (shown in the accompanying video). This

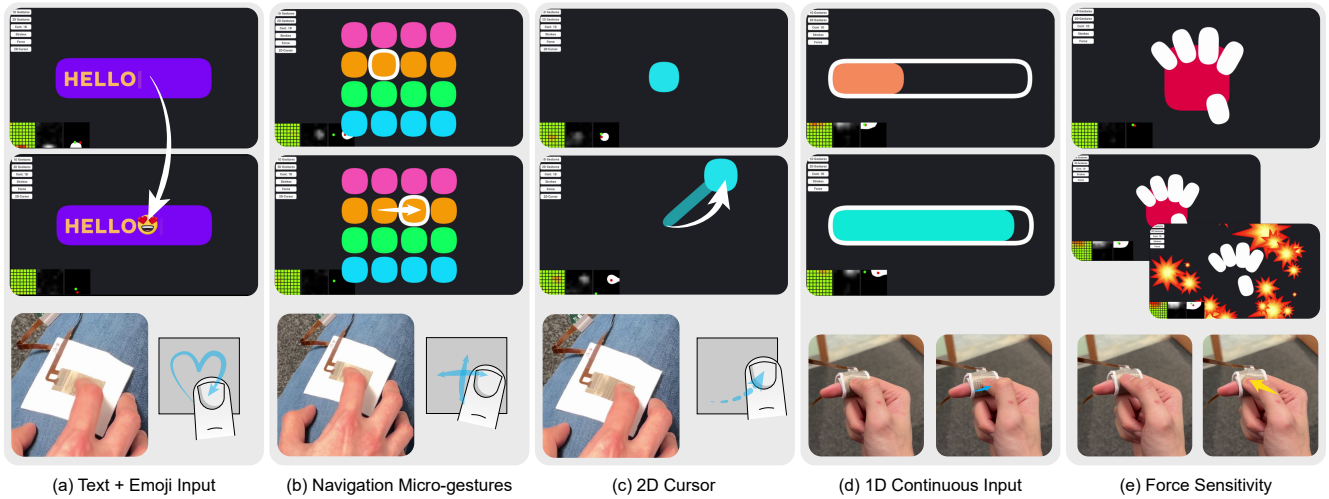

Figure 12: a) Text and emoji input using stroke-based gestures, b) Navigation and selection of a 2D grid of items using micro-gestures, c) Controlling a cursor using continuous 2D cursor control, d) 1-dimensional continuous input using the finger-sleeve prototype, e) Interaction showing force sensitivity for the finger-sleeve prototype

thumb-roll interaction can also be extended to navigation micro-gestures by triggering a gesture when a certain distance is passed instead of when the user lifts their thumb.

8.5 Force Sensitivity

All previous interactions introduced in this paper have used force (pressure and size) solely for stateful touch, which gates all subsequent interactions. In this demonstration, force is used for continuous input. The user is presented with a hand grasping a red ball (Figure 12e). As the user applies higher force the hand squeezes the red ball scaled to the amount of force. Once a threshold of force is reached, the hand starts to shake, if the user holds force above the threshold for 1 second, the ball explodes into confetti. This interaction is demonstrated on both the on-lap prototype and finger-sleeve prototype. This interaction can be extended further by introducing the concept of "force press" to the user as a new input gesture, which can be used as a contextual tap (akin to right-clicking on a computer system).

9 LIMITATIONS AND FUTURE WORK

High-throughput fabrication. The current fabrication methodology, which employs an automatic dispensing robot, is highly suitable for initial prototyping and personalized customization. To enhance yield and ensure consistent quality, integrating mass manufacturing techniques such as screen-printing for electrodes and molding for poly-islands on textiles can be beneficial.

Data acquisition and communications. Currently, data acquisition is tethered to a microcontroller and processed on a PC for extracting meaningful inputs from the sensor data. Integrating TouchpadAnyWear with actual wearable devices such as garments, gloves, wristbands, and watches, where the sensor data is processed on the device itself, could significantly expand the potential application space [17]. This will require reducing the electronics footprint and computational complexity but is well within reason since the current implementation does not require any costly computations such as deep neural networks.

Implementation for AR/VR/XR applications. As TouchpadAnyWear forms the basis of finger-based gestural input, and additionally as a general purpose high-resolution force sensor, there is high potential integration into AR/VR/XR applications. The robust capacitive sensing modality enhances reliability by mitigating issues such as environmental light interferences and view obstructions, commonly encountered with camera-based mid-air gesture inputs. Its seamless integration with textiles offers the possibility of transforming clothing or garments into natural wearable input interfaces, eliminating the need for additional accessories and promoting unobtrusive and ubiquitous interactions. Furthermore, enabling micro-gesture interactions with bare fingers at high spatial resolution facilitates discreet inputs when using smart AR/VR/XR equipment in public settings, thereby reducing social cognitive burdens and ensuring advanced user privacy protection.

10 CONCLUSION

This paper introduces TouchpadAnyWear, a novel family of universal wearable tactile sensors designed for sophisticated gesture inputs and recognition. This work addresses three critical challenges in textile sensors: achieving high spatial resolution, tolerance to motion artifacts, and seamless integration with textiles. We developed a textile-integrated capacitive-sensor architecture, where the knitted textile functions as an integral compressive core rather than merely a supportive substrate. The concept of "poly-islands" enables precise adjustment of the dielectric core's local stiffness through selective application of silicone onto the textiles. This regional programming of material modulus facilitates a strain-locking effect, ensuring that active sensing pixels remain insensitive to overall device deformation. Additionally, these textured "poly-islands"

provide passive tactile feedback, allowing users to locate sensing pixels for eyes-free interactions. Furthermore, we developed a scalable and customizable fabrication pipeline utilizing an automatic dispensing robot to create these poly-islands and stretchable electrodes. Finally, user study results have validated the efficacy of the textile touchpad and wearable finger sleeve in facilitating rich and intuitive human-computer interactions in daily life contexts.

ACKNOWLEDGMENTS

We express our gratitude for the help, assistance, and valuable discussions provided by our colleagues (listed in alphabetical order by last name): El Mehdi Abbara, Le Cai, Stuart Dealey, Joey Ellis, Cameron Glasscock, Li Guan, Jinjing Han, Rose Hope, Arpit Kalla, Sithika Ky, Tianshu Liu, Lawrence Own, Vanessa Sanchez, Simge Uzun, Xirong Wang, Sydney Wells, Eric Whitmire, Stefan Zelenovic. Additionally, we extend our thanks to all the volunteers who participated in our user studies.

REFERENCES

[1] Roland Aigner, Andreas Pointner, Thomas Preindl, Patrick Parzer, and Michael Haller. 2020. Embroidered resistive pressure sensors: A novel approach for textile interfaces. In *Proceedings of the 2020 CHI Conference on Human Factors in Computing Systems*. 1–13.

[2] Asli Atalay, Vanessa Sanchez, Ozgur Atalay, Daniel M Vogt, Florian Haufe, Robert J Wood, and Conor J Walsh. 2017. Batch fabrication of customizable silicone-textile composite capacitive strain sensors for human motion tracking. *Advanced Materials Technologies* 2, 9 (2017), 1700136.

[3] G. Bradski. 2000. The OpenCV Library. *Dr. Dobb's Journal of Software Tools* (2000).

[4] Tian Carey, Stefania Cacovich, Giorgio Divitini, Jiesheng Ren, Aida Mansouri, Jong M Kim, Chaoxia Wang, Caterina Ducati, Roman Sordan, and Felice Torrisi. 2017. Fully inkjet-printed two-dimensional material field-effect heterojunctions for wearable and textile electronics. *Nature communications* 8, 1 (2017), 1–11.

[5] Géry Casiez, Nicolas Roussel, and Daniel Vogel. 2012. 1€ filter: a simple speed-based low-pass filter for noisy input in interactive systems. In *Proceedings of the SIGCHI Conference on Human Factors in Computing Systems*. 2527–2530.

[6] Liwei Chan, Rong-Hao Liang, Ming-Chang Tsai, Kai-Yin Cheng, Chao-Huai Su, Mike Y. Chen, Wen-Huang Cheng, and Bing-Yu Chen. 2013. FingerPad: private and subtle interaction using fingertips. In *Proceedings of the 26th Annual ACM Symposium on User Interface Software and Technology* (St. Andrews, Scotland, United Kingdom) *(UIST '13)*. Association for Computing Machinery, New York, NY, USA, 255–260. https://doi.org/10.1145/2501988.2502016

[7] Tingyu Cheng, Zhihan Zhang, Bingrui Zong, Yuhui Zhao, Zekun Chang, Yejun Kim, Clement Zheng, Gregory D Abowd, and HyunJoo Oh. 2023. SwellSense: Creating 2.5 D interactions with micro-capsule paper. In *Proceedings of the 2023 CHI Conference on Human Factors in Computing Systems*. 1–13.

[8] Rajkumar Darbar, Prasanta Kr Sen, and Debasis Samanta. 2016. PressTact: Side pressure-based input for smartwatch interaction. In *Proceedings of the 2016 CHI Conference Extended Abstracts on Human Factors in Computing Systems*. 2431–2438.

[9] Sarah J Dempsey, Marek Szablewski, and Del Atkinson. 2015. Tactile sensing in human–computer interfaces: The inclusion of pressure sensitivity as a third dimension of user input. *Sensors and Actuators A: Physical* 232 (2015), 229–250.

[10] Minpyo Kang, Jejung Kim, Bongkyun Jang, Youngcheol Chae, Jae-Hyun Kim, and Jong-Hyun Ahn. 2017. Graphene-based three-dimensional capacitive touch sensor for wearable electronics. *ACS nano* 11, 8 (2017), 7950–7957.

[11] Hsin-Liu Kao, Artem Dementyev, Joseph A Paradiso, and Chris Schmandt. 2015. NailO: fingernails as an input surface. In *Proceedings of the 33rd Annual ACM Conference on Human Factors in Computing Systems*. 3015–3018.

[12] Thorsten Karrer, Moritz Wittenhagen, Leonhard Lichtschlag, Florian Heller, and Jan Borchers. 2011. Pinstripe: eyes-free continuous input on interactive clothing. In *Proceedings of the SIGCHI Conference on Human Factors in Computing Systems*. 1313–1322.

[13] Daehwa Kim and Chris Harrison. 2022. EtherPose: Continuous hand pose tracking with wrist-worn antenna impedance characteristic sensing. In *Proceedings of the 35th Annual ACM Symposium on User Interface Software and Technology*. 1–12.

[14] David Kim, Otmar Hilliges, Shahram Izadi, Alex D Butler, Jiawen Chen, Iason Oikonomidis, and Patrick Olivier. 2012. Digits: freehand 3D interactions anywhere using a wrist-worn gloveless sensor. In *Proceedings of the 25th annual ACM symposium on User interface software and technology*. 167–176.

[15] Riku Kitamura, Takumi Yamamoto, and Yuta Sugiura. 2023. TouchLog: Finger Micro Gesture Recognition Using Photo-Reflective Sensors. In *Proceedings of the 2023 ACM International Symposium on Wearable Computers*. 92–97.

[16] Jacob Kornerup and Taylor Hall. 1994. *Mapping powerlists onto hypercubes*. Univ., Department of Computer Sciences.

[17] Weilun Li, Zhili Xiao, Junyi Zhao, Kenji Aono, Stephanie Pizzella, Zichao Wen, Yong Wang, Chuan Wang, and Shantanu Chakrabartty. 2023. A portable and a scalable multi-channel wireless recording system for wearable electromyometrial imaging. *IEEE Transactions on Biomedical Circuits and Systems* (2023).

[18] Weilun Li, Junyi Zhao, Yong Wang, Chuan Wang, and Shantanu Chakrabartty. 2024. A Low-Power Impedance-to-Frequency Converter for Frequency-Multiplexed Wearable Sensors. *IEEE Transactions on Biomedical Circuits and Systems* (2024).

[19] Li-Wei Lo, Junyi Zhao, Kenji Aono, Weilun Li, Zichao Wen, Stephanie Pizzella, Yong Wang, Shantanu Chakrabartty, and Chuan Wang. 2022. Stretchable sponge electrodes for long-term and motion-artifact-tolerant recording of high-quality electrophysiologic signals. *ACS nano* 16, 8 (2022), 11792–11801.

[20] Li-Wei Lo, Junyi Zhao, Haochuan Wan, Yong Wang, Shantanu Chakrabartty, and Chuan Wang. 2021. An inkjet-printed PEDOT: PSS-based stretchable conductor for wearable health monitoring device applications. *ACS Applied Materials & Interfaces* 13, 18 (2021), 21693–21702.

[21] Li-Wei Lo, Junyi Zhao, Haochuan Wan, Yong Wang, Shantanu Chakrabartty, and Chuan Wang. 2022. A soft sponge sensor for multimodal sensing and distinguishing of pressure, strain, and temperature. *ACS Applied Materials & Interfaces* 14, 7 (2022), 9570–9578.

[22] Yiyue Luo, Kui Wu, Tomás Palacios, and Wojciech Matusik. 2021. KnitUI: Fabricating interactive and sensing textiles with machine knitting. In *Proceedings of the 2021 CHI Conference on Human Factors in Computing Systems*. 1–12.

[23] Yiyue Luo, Junyi Zhu, Kui Wu, Cedric Honnet, Stefanie Mueller, and Wojciech Matusik. 2023. MagKnitic: Machine-knitted Passive and Interactive Haptic Textiles with Integrated Binary Sensing. In *Proceedings of the 36th Annual ACM Symposium on User Interface Software and Technology*. 1–13.

[24] Eric J Markvicka, Michael D Bartlett, Xiaonan Huang, and Carmel Majidi. 2018. An autonomously electrically self-healing liquid metal–elastomer composite for robust soft-matter robotics and electronics. *Nature materials* 17, 7 (2018), 618–624.

[25] Jagan Singh Meena, Su Bin Choi, Tran Duc Khanh, Hyun Sik Shin, Jun Sang Choi, Jinho Joo, and Jong-Woong Kim. 2023. Highly stretchable and robust textile-based capacitive mechanical sensor for human motion detection. *Applied Surface Science* 613 (2023), 155961.

[26] Viet Nguyen, Siddharth Rupavatharam, Luyang Liu, Richard Howard, and Marco Gruteser. 2019. HandSense: capacitive coupling-based dynamic, micro finger gesture recognition. In *Proceedings of the 17th Conference on Embedded Networked Sensor Systems* (New York, New York) *(SenSys '19)*. Association for Computing Machinery, New York, NY, USA, 285–297. https://doi.org/10.1145/3356250.3360040

[27] Farshid Salemi Parizi, Eric Whitmire, and Shwetak Patel. 2019. Auraring: Precise electromagnetic finger tracking. *Proceedings of the ACM on Interactive, Mobile, Wearable and Ubiquitous Technologies* 3, 4 (2019), 1–28.

[28] Pornthep Preechayasomboon. [n. d.]. *Bricklayer - Experiment Structures for User Studies in Unity*. https://github.com/prnthp/experiment-structures

[29] Christian Rendl, Patrick Greindl, Kathrin Probst, Martin Behrens, and Michael Haller. 2014. Presstures: exploring pressure-sensitive multi-touch gestures on trackpads. In *Proceedings of the SIGCHI conference on human factors in computing systems*. 431–434.

[30] Mohamed Soliman, Franziska Mueller, Lena Hegemann, Joan Sol Roo, Christian Theobalt, and Jürgen Steimle. 2018. FingerInput: Capturing Expressive Single-Hand Thumb-to-Finger Microgestures. In *Proceedings of the 2018 ACM International Conference on Interactive Surfaces and Spaces* (Tokyo, Japan) *(ISS '18)*. Association for Computing Machinery, New York, NY, USA, 177–187. https://doi.org/10.1145/3279778.3279799

[31] Paul Strohmeier, Jarrod Knibbe, Sebastian Boring, and Kasper Hornbæk. 2018. zPatch: Hybrid resistive/capacitive etextile input. In *Proceedings of the Twelfth International Conference on Tangible, Embedded, and Embodied Interaction*. 188–198.

[32] Hsin-Ruey Tsai, Cheng-Yuan Wu, Lee-Ting Huang, and Yi-Ping Hung. 2016. ThumbRing: private interactions using one-handed thumb motion input on finger segments. In *Proceedings of the 18th International Conference on Human-Computer Interaction with Mobile Devices and Services Adjunct* (Florence, Italy) *(MobileHCI '16)*. Association for Computing Machinery, New York, NY, USA, 791–798. https://doi.org/10.1145/2957265.2961859

[33] Radu-Daniel Vatavu, Lisa Anthony, and Jacob O Wobbrock. 2018. $Q: A super-quick, articulation-invariant stroke-gesture recognizer for low-resource devices. In *Proceedings of the 20th International Conference on Human-Computer Interaction with Mobile Devices and Services*. 1–12.

[34] Chi Cuong Vu and Jooyong Kim. 2020. Simultaneous sensing of touch and pressure by using highly elastic e-fabrics. *Applied Sciences* 10, 3 (2020), 989.

[35] Anandghan Waghmare, Youssef Ben Taleb, Ishan Chatterjee, Arjun Narendra, and Shwetak Patel. 2023. Z-Ring: Single-Point Bio-Impedance Sensing for Gesture,

Touch, Object and User Recognition. In *Proceedings of the 2023 CHI Conference on Human Factors in Computing Systems*. 1–18.

[36] Martin Weigel, Tong Lu, Gilles Bailly, Antti Oulasvirta, Carmel Majidi, and Jürgen Steimle. 2015. Iskin: flexible, stretchable and visually customizable on-body touch sensors for mobile computing. In *Proceedings of the 33rd Annual ACM Conference on Human Factors in Computing Systems*. 2991–3000.

[37] Eric Whitmire, Mohit Jain, Divye Jain, Greg Nelson, Ravi Karkar, Shwetak Patel, and Mayank Goel. 2017. Digitouch: Reconfigurable thumb-to-finger input and text entry on head-mounted displays. *Proceedings of the ACM on Interactive, Mobile, Wearable and Ubiquitous Technologies* 1, 3 (2017), 1–21.

[38] Anusha Withana, Daniel Groeger, and Jürgen Steimle. 2018. Tacttoo: A thin and feel-through tattoo for on-skin tactile output. In *Proceedings of the 31st Annual ACM Symposium on User Interface Software and Technology*. 365–378.

[39] Jianguo Xi, Huaiwen Yang, Xinyu Li, Ruilai Wei, Taiping Zhang, Lin Dong, Zhenjun Yang, Zuqing Yuan, Junlu Sun, and Qilin Hua. 2024. Recent Advances in Tactile Sensory Systems: Mechanisms, Fabrication, and Applications. *Nanomaterials* 14, 5 (2024), 465.

[40] Ruidong Xu, Minghua She, Jiaxu Liu, Shikang Zhao, Jisheng Zhao, Xueji Zhang, Lijun Qu, and Mingwei Tian. 2023. Skin-friendly and wearable iontronic touch panel for virtual-real handwriting interaction. *ACS nano* 17, 9 (2023), 8293–8302.

[41] Zheer Xu, Pui Chung Wong, Jun Gong, Te-Yen Wu, Aditya Shekhar Nittala, Xiaojun Bi, Jürgen Steimle, Hongbo Fu, Kening Zhu, and Xing-Dong Yang. 2019. Tiptext: Eyes-free text entry on a fingertip keyboard. In *Proceedings of the 32nd Annual ACM Symposium on User Interface Software and Technology*. 883–899.

[42] Guang Yang, Renquan Xing, Yafang Li, Chongqi Ma, Bowen Cheng, Jing Yan, and Xupin Zhuang. 2021. Toward high-performance multifunctional electronics: Knitted fabric-based composite with electrically conductive anisotropy and self-healing capacity. *Chemical Engineering Journal* 426 (2021), 131931.

[43] Shanshan Yao, Ji Yang, Felipe R Poblete, Xiaogang Hu, and Yong Zhu. 2019. Multifunctional electronic textiles using silver nanowire composites. *ACS applied materials & interfaces* 11, 34 (2019), 31028–31037.

[44] Sang Ho Yoon, Ke Huo, Vinh P Nguyen, and Karthik Ramani. 2015. TIMMi: Finger-worn textile input device with multimodal sensing in mobile interaction. In *Proceedings of the Ninth International Conference on Tangible, Embedded, and Embodied Interaction*. 269–272.

[45] Sang Ho Yoon, Ke Huo, and Karthik Ramani. 2014. Plex: finger-worn textile sensor for mobile interaction during activities. In *Proceedings of the 2014 ACM International Joint Conference on Pervasive and Ubiquitous Computing: Adjunct Publication*. 191–194.

[46] Yang Zhang, Junhan Zhou, Gierad Laput, and Chris Harrison. 2016. Skintrack: Using the body as an electrical waveguide for continuous finger tracking on the skin. In *Proceedings of the 2016 CHI Conference on Human Factors in Computing Systems*. 1491–1503.

[47] Zhihan Zhang, Mallory Parker, Kuotian Liao, Jerry Cao, Anandghan Waghmare, Joseph Breda, Chris Matsumura, Serena Eley, Eleftheria Roumeli, Shwetak Patel, and Vikram Iyer. 2024. Biodegradable Interactive Materials. arXiv:2404.03130 [cs.HC] https://arxiv.org/abs/2404.03130

[48] Junyi Zhao, Chansoo Kim, Weilun Li, Zichao Wen, Zhili Xiao, Yong Wang, Shantanu Chakrabartty, and Chuan Wang. 2024. 3D E-textile for Exercise Physiology and Clinical Maternal Health Monitoring. arXiv:2407.07954 [physics.med-ph] https://arxiv.org/abs/2407.07954

[49] Junyi Zhao, Li-Wei Lo, Haochuan Wan, Pengsu Mao, Zhibin Yu, and Chuan Wang. 2021. High-Speed Fabrication of All-Inkjet-Printed Organometallic Halide Perovskite Light-Emitting Diodes on Elastic Substrates. *Advanced Materials* 33, 48 (2021), 2102095.

[50] Junyi Zhao, Li-Wei Lo, Zhibin Yu, and Chuan Wang. 2023. Handwriting of perovskite optoelectronic devices on diverse substrates. *Nature Photonics* 17, 11 (2023), 964–971.

[51] Mengjia Zhu, Amirhossein H Memar, Aakar Gupta, Majed Samad, Priyanshu Agarwal, Yon Visell, Sean J Keller, and Nicholas Colonnese. 2020. Pneusleeve: In-fabric multimodal actuation and sensing in a soft, compact, and expressive haptic sleeve. In *Proceedings of the 2020 CHI conference on human factors in computing systems*. 1–12.